Preclinical evaluation of taxane-binding peptide-modified polymeric micelles loaded with docetaxel in an orthotopic breast cancer mouse model

CrossMark

Jennifer Logie [a], Ahil N. Ganesh [a], Ahmed M. Aman [b], Rima S. Al-awar [b], Molly S. Shoichet [a, c, *]

[a] Terrence Donnelly Centre for Cellular and Biomolecular Research, Department of Chemical Engineering & Applied Chemistry, Institute of Biomaterials & Biomedical Engineering, University of Toronto, Room 514, 160 College Street, Toronto, ON M5S 3E1, Canada
[b] Medicinal Chemistry, Ontario Institute for Cancer Research, 101 College Street, Toronto, ON M5G 1L7, Canada
[c] Department of Chemistry, University of Toronto, 80 St. George Street, Toronto, ON M5S 3H6, Canada

ARTICLE INFO

ABSTRACT

We developed a novel taxane-binding peptide (TBP) modified, biodegradable polymeric micelle that overcomes limitations of drug loading and poor serum stability typically seen with particle delivery, leading to enhanced pharmacokinetics and tumor distribution of docetaxel (DTX). The use of the taxane-binding peptide to increase docetaxel loading is particularly compelling as it takes advantage of a known intracellular binding mechanism in a new way. Docetaxel is a potent chemotherapeutic with a therapeutic index often limited by the toxicity of the excipients that are necessary to enhance its solubility for intravenous delivery. Our polymeric micelle has terminal furan groups that enable facile antibody Fab conjugation by Diels-Alder chemistry for targeted delivery. Compared to the conventional ethanolic polysorbate 80 formulation (Free DTX), our nanoparticle (NP DTX) formulation exhibited a two-fold increase in exposure and tumor accumulation. Notably, the reduced toxicity of the NP DTX formulation increased the therapeutic index and allowed for higher dosing regimens, with a maximum tolerated dose (MTD) 1.6-fold higher than that of the Free DTX formulation, which is significant and similar to enhancements observed in clinical products for docetaxel and other drugs. These improved properties led to enhanced mouse survival in an orthotopic model of breast cancer; however, the targeted formulation of Fab-NP DTX did not further improve efficacy. Together, these results clearly demonstrate the benefits of the TBP-modified polymeric micelles as promising carriers for docetaxel.

© 2017 Published by Elsevier Ltd.

1. Introduction

Despite widespread clinical use, taxane chemotherapeutics, like docetaxel (DTX), represent a formulation challenge. Current clinical formulations have dose-limiting systemic side effects, such as neutropenia [1] and hypersensitivity reactions [2] associated with the high concentrations of undesirable excipients (e.g. polysorbate 80). To circumvent these issues, nanoparticle delivery strategies have been pursued with biocompatible amphiphilic polymers that solubilize drugs within their hydrophobic core during self-assembly.

While several polymeric micelle strategies have been explored, these systems are plagued by low drug loadings and poor stability that can limit their translation in vivo [3—5]. By facilitating inter-molecular interactions within the micelle core, high drug loadings and stability in serum conditions can be achieved [6—9]. Furthermore, enhanced drug-carrier compatibility has been shown to improve nanotherapy efficacy [10,11]. Our novel polymer, poly(D,L-lactide-co-2-methyl-2-carboxytrimethylene carbonate)-graft-polyethylene glycol (P(LA-co-TMCC)-g-PEG, Fig. 1A), forms stable micelles, and is amenable to chemical modification through carboxylic acids along the backbone and end group PEG modification

on the corona [12,13]. In order to increase docetaxel (DTX) loading, we incorporated the taxane-binding peptide (TBP) into our polymer design, thereby taking advantage of a known intracellular binding pathway. We achieved twice as much loaded DTX in our polymeric micelles than typical nanoparticle formulations with linear copolymers [6]. Notably, this docetaxel-micelle system was stable against dissociation and drug release in serum with a half-life greater than 24 h [6].

Herein, we test the in vivo efficacy of this new polymeric micelle formulation (P_TBP) with encapsulated DTX and evaluate the utility of active targeting with the incorporation of a novel anti-human epidermal growth factor receptor 2 (HER2) fragment antibody, Fab 73J (Fig. 1B). The use of Fab has been shown to mitigate the premature clearance associated with antibody engagement of Fcγ receptors on immune cells [14]. Compared to the clinically used trastuzumab, Fab 73J binds to a unique epitope of the HER2 receptor and has comparable binding and trafficking [15].

We assessed the preclinical efficacy of this formulation in a clinically relevant orthotopic tumor model. In the current study, we used an established orthotopic breast cancer model in NOD-SCID-IL-2Rγnull (NSG) mice to better recapitulate the human disease [16]. Compared to subcutaneous xenograft models, orthotopic models more accurately represent the vasculature and metastatic potential of patient tumors and better predict clinical results [16–20]. Here we report the enhanced tolerability and efficacy of a taxane-binding peptide conjugated polymeric micelle formulation of DTX in this mouse model of breast cancer.

2. Results

2.1. Synthesis and characterization of NP DTX

The polymers used to prepare nanoparticles (NP DTX) were synthesized by an organocatalyzed ring opening polymerization of D,L-lactide (LA) and 5-methyl-5-benzyloxycarbonyl-1,3-trimethylene carbonate (TMCC-Bn) followed by benzyl deprotection to produce the poly(D,L-lactide-co-2-methyl-2-carboxytrimethylene carbonate) (P(LA-co-TMCC)) backbone [21] that was then grafted with 10,000 g/mol PEG chains by carbodiimide chemistry [22]. Polymers were characterized by ^{1}H NMR and showed an average of 3 PEGs/backbone. P(LA-co-TMCC)-g-PEG-furan (P_furan) was synthesized by grafting furan-terminated PEG while P(LA-co-TMCC)-g-PEG, TBP (P_TBP) was synthesized by grafting methoxy-terminated PEG. P_TBP was synthesized by Michael addition between the maleimide-TBP peptide and a thiolated backbone, and showed an average of 1 peptide/backbone by amino acid analysis [6]. NP DTX was formed by co-dissolving polymers (10% P_furan, 90% P_TBP) and docetaxel in DMF and then dialyzing against water for 24 h. The Z-average particle size was measured by dynamic light scattering (DLS) to be 121 ± 25 nm with a distribution of 0.15 ± 0.03. The particle size is larger than particles without docetaxel (108 ± 16 nm), consistent with observations from other systems [11,23]. Absolute drug loading of particles used in the three in vivo studies was $18.5 \pm 1.1\%$, which is double that achieved by any other micellar formulations of docetaxel [24,25] and reflects the importance of the incorporation of the taxane-binding peptide to drug loading.

To assess the benefit of actively targeting the cancer cells, we
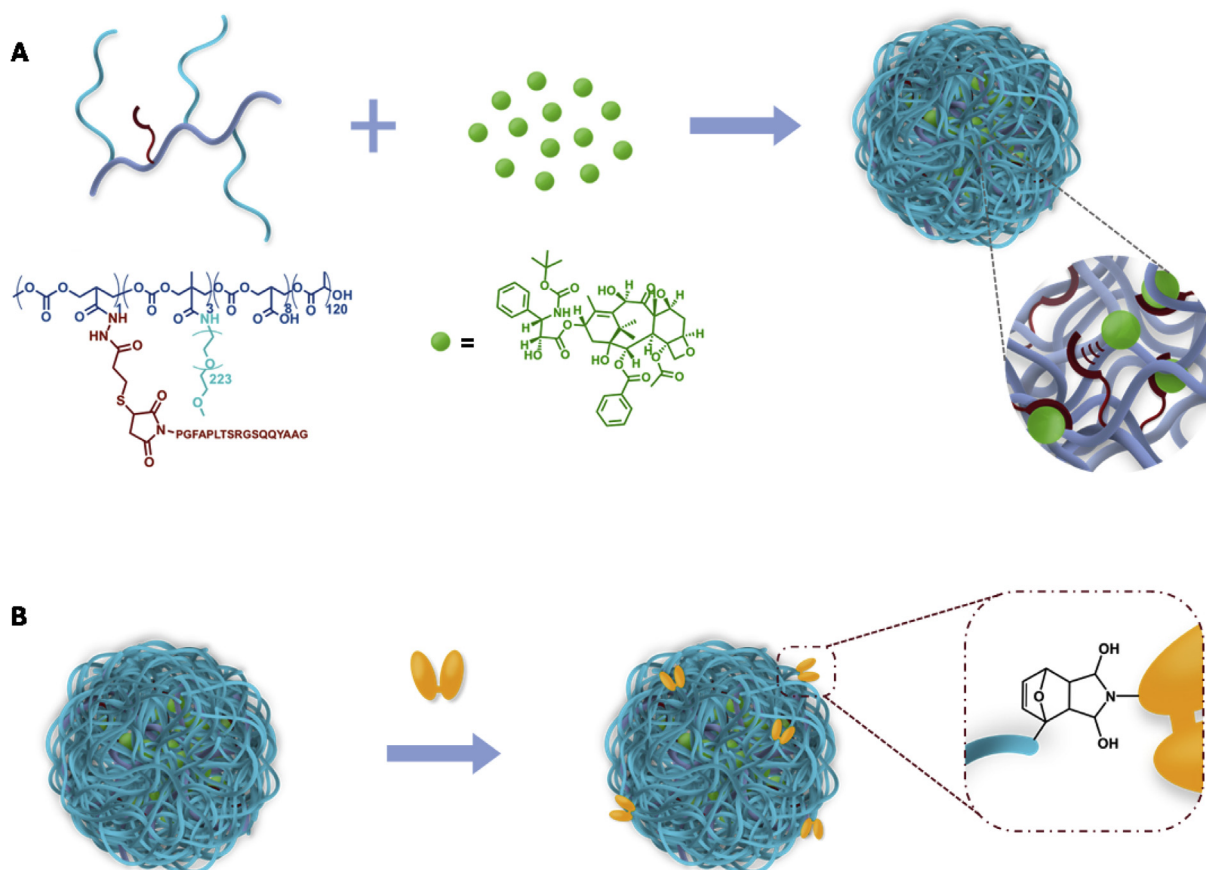
Fig. 1. (A) Schematic of NP DTX formation from self-assembly of P_TBP (P(LA-co-TMCC)-g-PEG,TBP) with docetaxel. Docetaxel binds specifically to TBP, facilitating high drug loading. (B) Fab 73J conjugation to NP by furan-maleimide Diels-Alder click chemistry with P_furan (P(LA-co-TMCC)-g-PEG-furan).

included a targeted arm in our efficacy study. NP DTX was targeted by conjugating Fab 73J, a novel HER2-binding Fab, using Diels-Alder click chemistry between the furan end groups of the PEG and maleimide-modified Fab 73J to achieve an average of 10 Fab/NP (Fig. 1B). The Fab 73J increases intracellular uptake of NPs in vitro in HER2+ breast cancer cell lines relative to trastuzumab as determined by in vitro confocal imaging [15].

2.2. Maximum tolerated dose

Before evaluating the pharmacokinetics and efficacy of our formulation, we evaluated its tolerability compared to a clinically relevant surfactant-based formulation. Taxotere, the clinically used formulation of docetaxel, is comprised of docetaxel in a solution of 20% polysorbate 80 and 13% ethanol in saline, which is diluted and delivered over a 3 h infusion in patients. As this formulation caused severe toxicity upon bolus injection into the NSG mice, we reduced the excipients to 7.5% polysorbate 80 and 12.5% ethanol for the Free DTX formulation in this study. Even this scaled-down formulation caused mild lethargy immediately following injection in many of the animals. In contrast, injections of NP DTX and NP alone (i.e., particles without docetaxel) caused no adverse reaction upon injection, and injection of NP alone was comparable to that of no injection in terms of animal activity level and tail vein damage.

Strikingly, the maximum tolerated dose (MTD) of DTX was 1.6-times higher in the NP DTX formulation compared to the free formulation (8 mg/kg vs. 5 mg/kg, Fig. S1). Significant weight loss (>20%) was seen in animals receiving high doses of Free DTX (>5 mg/kg). In contrast, NP DTX up to 8 mg/kg caused only minor weight loss (<10%) and a rapid 3−5 d recovery without any abnormality in the histology (data not shown) of clearance organs, such as the kidney and liver. The number of injections was limited to three due to severe tail vein damage from the high percentage of polysorbate 80 (7.5%) used in the Free DTX formulation. The improved tolerability of the NP DTX formulation gives a greater therapeutic index and allows for higher dosing in the efficacy study. Before assessing the efficacy, we characterized the two formulations in terms of pharmacokinetics and biodistribution.

2.3. Pharmacokinetics & biodistribution

Pharmacokinetics and biodistribution of NP DTX and DTX formulations were evaluated at the MTD of the free drug formulation (5 mg/kg), thereby allowing the two formulations to be compared at equivalent doses. Following a bolus intravenous injection, docetaxel quickly distributes through the body and is metabolized and eliminated. Consistent with previously reported pharmacokinetic profiles of this drug [26,27], both the free and NP formulations show a significant drop in plasma concentration immediately following injection, with less than 10% of the initial dose remaining in the plasma after 10 min (Fig. 2). NP DTX showed a modest improvement in pharmacokinetic parameters over the 7 h time period. The lambda half-life ($t_{1/2,\lambda}$) of the drug in the plasma showed a 1.5-fold increase. The area-under-the-curve (AUC), a measure of drug exposure, had a 2-fold increase while the clearance (Cl), a measure of drug elimination, was reduced to half of that of the conventional formulation (Fig. 2). Interestingly, these seemingly modest improvements show enhancement in pharmacokinetics and tolerated dose compared to those seen with clinically used NP formulations of paclitaxel such as Genexol-PM [28] and Nanoxel-PM, a docetaxel formulation currently under evaluation [29]. Importantly, these parameters suggest greater drug exposure to the tumor at equivalent doses, and the extended circulation time enables greater tumor accumulation.

To evaluate biodistribution, a panel of organs was harvested at

sacrificial time points between 1 and 24 h. DTX was quantified after extraction from tissue by HPLC-MS/MS. While nanoparticles frequently accumulate in organs of the mononuclear phagocyte system, such as the liver or spleen, no significant differences were seen between the NP and conventional formulation. With the exception of the 1 h time point, the distribution was similar between the two formulations in the liver, spleen, kidney, heart and lungs (Fig. 3). In the liver we see the drug is rapidly washed out or metabolized, with <0.1% of the initial dose present at the 24 h time point. The other organs show a sharp decline in DTX concentration over the 24 h, consistent with clearance from these organs. Interestingly, reduction in DTX content in the tumor tissue was more gradual, with NP DTX formulations maintaining approximately 1% of the initial dose at the 24 h time point. The tumor tissue showed increased accumulation (between 1.7 and 2.8-times between 2 and 8 h) of DTX at early time points when delivered in the NP formulation vs. in the free form, suggesting passive targeting to the tumor site of NP DTX.

2.4. Efficacy in MDA-MB-231/H2N tumor model

We used an orthotopic HER2+ breast cancer model in NSG mice to evaluate the anti-tumor efficacy of systemically administered NP DTX compared to both actively targeted Fab-NP DTX and Free DTX. When tumors were palpable, with an average volume of 10 mm^3, mice were administered three doses (at days 0, 5, and 8 after palpable tumors) of either NP alone, 5 mg/kg Free DTX, 5 mg/kg NP DTX, 8 mg/kg NP DTX or 8 mg/kg Fab-NP DTX. By comparing the maximum tolerated dose of Free DTX (5 mg/kg) to the same dose of NP DTX and to the maximum tolerated dose of NP DTX (8 mg/kg), we gained a better understanding of the benefit of NP DTX. Furthermore by comparing the NP DTX to the Fab-NP DTX, we gained a better understanding of the benefit of active targeting. On Day 39, both Free and NP DTX at 5 mg/kg significantly inhibited tumor growth by 50% compared to the NP alone group (p < 0.001, Fig. 4A and S2). At 8 mg/kg, inhibition of growth was more pronounced than the lower dose, with both NP DTX and Fab-NP DTX formulations significantly inhibiting growth by 72% compared to NP alone and 48% compared to the lower dose (p < 0.001). Importantly, this difference was seen over a month after injection, suggesting that long-term tumor growth was reduced with early treatment. While in this immunocompromised NSG model we did not expect additional toxicity associated with the 73JFab, we did expect enhanced efficacy at the tumor associated with targeting to HER2. There was no difference in Fab-NP DTX and NP DTX, indicating that the 73JFab had minimal impact on DTX tumor targeting. Notably, no visible signs of distress were detected in mice treated with NP DTX at either dose and the limited weight loss observed (Fig. 4B) showed good tolerability of these selected doses over the 60-day study period. The improved tolerability of the NP DTX formulation correlated with better survival due to higher dosing, with animals receiving 8 mg/kg NP DTX living an average of 30% longer than those receiving Free DTX drug at 5 mg/kg (p < 0.001, Mantel-Cox test, Fig. 4C).

3. Discussion

Polymeric micelles for chemotherapeutic delivery are frequently limited by their low loading and poor stability in vivo. By modifying the polymeric backbone with the taxane-binding peptide, high drug loading is achieved without loss of micelle stability. This high loading facilitates efficacious doses of docetaxel to be delivered in vivo with 2-fold lower polymer concentrations than typical NP systems. This NP formulation is tolerated better than the conventional surfactant based formulation, increasing the maximum
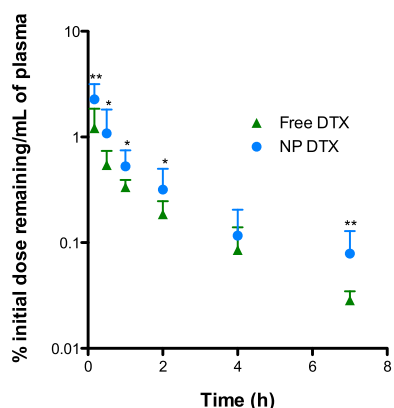
Parameter	Free DTX	NP DTX
$t_{1/2, \lambda}$	1.69 h	2.29 h
AUC (to t=7h)	1730 h ng^{-1}mL^{-1}	3100 h ng^{-1} mL^{-1}
Cl	1940 mL h^{-1} kg^{-1}	1060 mL h^{-1} kg^{-1}

Fig. 2. Pharmacokinetic profiles of Free DTX and NP DTX in tumor bearing mice. Plasma concentration is significantly higher in the NP DTX formulation at all time points except for 4 h (where there is no statistical difference), and gives a higher half-life, $t_{1/2, \lambda}$ (1.5x greater), area under the curve, AUC (2x greater) and slower clearance, Cl (~50% slower) (n = 10, mean + SD, *p < 0.05, **p < 0.01).
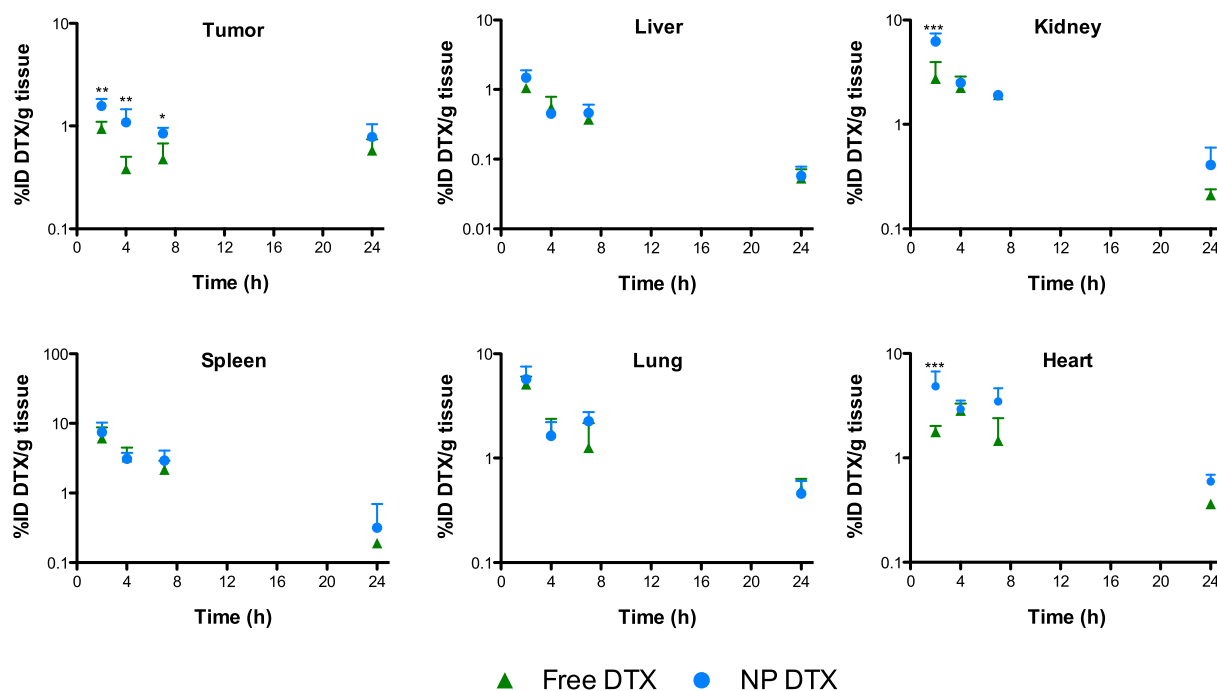
Fig. 3. Biodistribution profiles of Free DTX and NP DTX in tumor, liver, kidney, spleen, lung and heart at 4 time points. The tumor shows increased accumulation of DTX when delivered in NP DTX formulation at early time points (n = 3, mean + SD, *p < 0.05, **p < 0.01, ***p < 0.001).

tolerated dose from 5 mg/kg to 8 mg/kg; this increase of 1.6-times had a dramatic effect in vivo. While there are currently no FDA-approved nanoparticle formulations of docetaxel, formulations of other chemotherapeutics have been approved as first-line therapy for a range of cancers (e.g. Abraxane, Marqibo, Genexol-PM and Doxil) [30]. Enhanced tolerability has proven crucial to the clinical success of these nanoparticles [28], with all of the clinical formulations being given approval on the basis of improving the drug's toxicological profile in patients [31,32]. Many of these nanoparticles have also improved clinical outcomes of drugs due to increased dosing and favorable pharmacokinetic profiles. Notably, the delivery of paclitaxel in a nanoparticle (Abraxane) allowed a 1.7-fold increase of the maximum tolerated dose over Taxol, and showed a significantly better response rate (33% versus 19%) in a Phase III trial in breast cancer patients [33].

The rationale behind many NP delivery strategies is based on tumor accumulation due to the enhanced permeability and retention (EPR) effect [34]. This has become a widely debated area, as the translation of NPs to humans has been hampered due to tumor heterogeneity between patients and cancers [35]. Clinical results suggest that the EPR effect is not consistent, and only a subset of patients may benefit from the use of vehicles on the nanoscale [36,37]. Notwithstanding these observations, the value of NP platforms extends beyond the EPR effect. Successful solubilization of the hydrophobic drug in biocompatible carriers can improve the therapeutic index and enhance tumor accumulation [38]. Our novel taxane-binding peptide-conjugated particle platform showed improvements in pharmacokinetics compared to the free formulation, with an increase in parameters indicative of drug exposure, such as half-life and area-under-the-curve, and a decrease in parameters indicative of drug elimination, such as the clearance. Additionally, we see enhanced tumor accumulation at early time points up to 8 h, similar to improvements seen with other carriers of taxanes, such as Genexol-PM [28]. While other
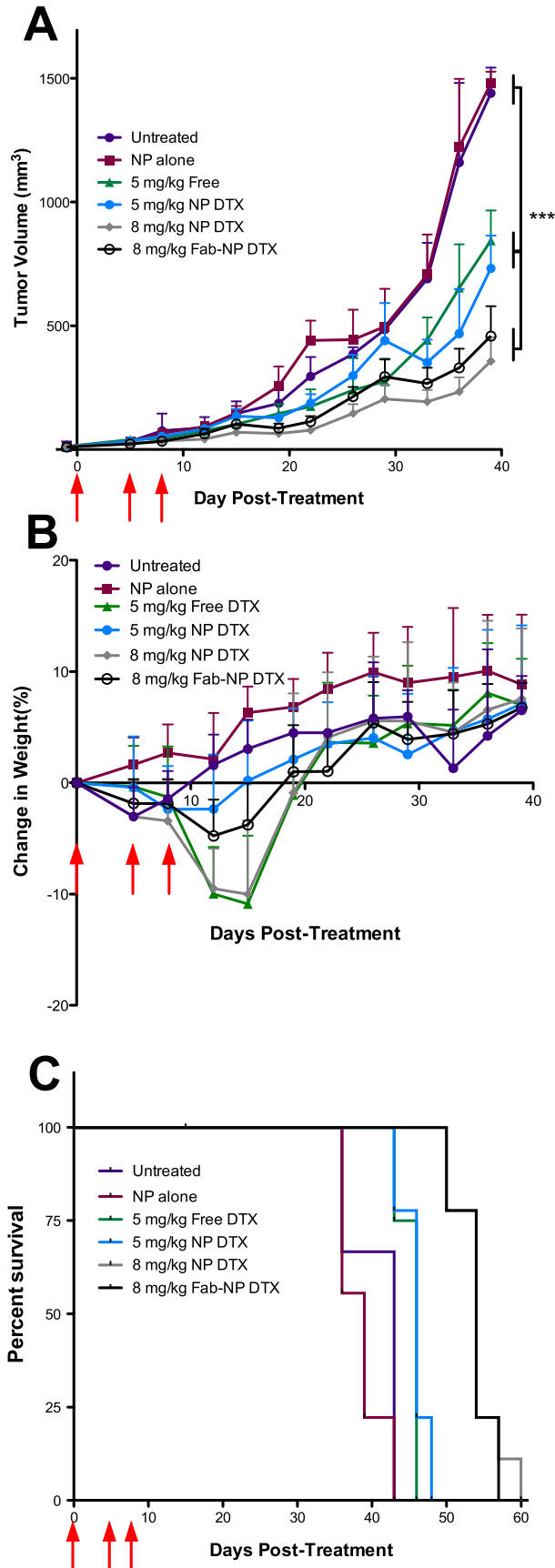
Fig. 4. Efficacy of NP DTX in MDA-MB-231/H2N bearing NSG mice. (A) Anti-tumor effect of NP DTX (with or without Fab73J, 5 mg/kg or 8 mg/kg) compared to Free

carriers show greater exposure and half-life [11,27], since severe neutropenia and thrombocytopenia are the main side effects of this drug [1], the modest enhancements in the plasma $t_{1/2}$ that we observe are likely more desirable for future translation. Remarkably, there was no significant enhancement of DTX levels in the organs of the mononuclear phagocyte system (MPS), the liver and spleen, suggesting that the highly PEGylated surface was able to successfully modulate the MPS response [22,39].

Our novel NP DTX platform was efficacious against an orthotopic HER2$^+$ breast cancer tumor in NSG mice, showing a reduced tumor burden compared to NP alone. Importantly, the heightened tolerability of this formulation allowed higher doses than the surfactant based formulation, resulting in reduced tumor size and longer survival. Previous NP formulations of DTX, such as Nanoxel-PM, show similar maximum tolerated doses to the surfactant based formulation of free DTX [29], which is significantly less than that achieved herein.

It should be noted that while orthotopic models have been shown to be more clinically relevant [17,18], they also require the use of severely immunocompromised mouse strains, such as the NSG, whose sensitivity reduces tolerability for chemotherapeutics. The challenge of these models is that we do not see the sought-after complete tumor regression, which has been achieved in other mouse strains; however, the significant reduction in tumor burden that we observed over the course of the study is promising [40]. Importantly, tumor response alone is not a good endpoint and does not always correlate with overall survival [35]. For this reason, we also show that high doses of NP DTX can extend survival of animals by over 30% compared to the maximum tolerated dose of Free DTX. At matched doses, there are no significant differences between NP DTX and Free DTX in terms of tumor size and survival, suggesting that the enhancements in PK and biodistribution of NP DTX do not correlate to an improvement in efficacy. While tumor sizes are smaller for dose-matched NP DTX at most time points, these differences are not significant. This result is similar to a recent study by Yan et al., where paclitaxel delivered in NPs showed improvement based on tolerability, but not in tumor burden at matched doses [41].

The utility of the Fab 73J targeting ligand is of particular interest. We chose the Fab vs. the full IgG to minimize the immune response to the Fc region, even though we recognize that this would have minimal (if any) impact in the NSG mouse model. While previous in vitro studies [15] showed that the incorporation of an active targeting ligand increases cell uptake, this did not result in improved efficacy in vivo. There were no significant differences between Fab-NP DTX and NP DTX at matched doses, suggesting that the incorporation of the Fab does not impact efficacy in this system. This is consistent with a number of previous reports, which suggest that, for the delivery of hydrophobic small molecules which freely penetrate cell membranes when released from their vehicle, active targeting ligands provide no additional benefit [42–45]. While ligands are able to efficiently get NPs into cancer cells in vitro, they neither change the in vivo biodistribution nor the tumor accumulation [46,47]. It should be noted that active targeting ligands could have significant value for

DTX (5 mg/kg). Higher (8 mg/kg) doses of NP DTX resulted in significant inhibition of tumor growth compared to controls and Free DTX at 5 mg/kg (p < 0.001). (n = 9, except for untreated n = 3, mean + SD). (B) Weight loss showed good tolerability of all formulations (maximum weight loss was ~10%) with recovery within 5 days. (n = 9, except for untreated n = 3, mean + SD). Red arrows indicate injections of specified treatments. (C) Kaplan-Meier survival plots correlate to tumor growth plot, showing high doses of NP DTX allow survival up to 60 d after the initial injection. (For interpretation of the references to colour in this figure legend, the reader is referred to the web version of this article.)

the delivery of hydrophilic therapeutics, such as siRNA, which cannot passively diffuse across membranes [48,49]. They also have utility when the antibody has therapeutic efficacy, as in antibody-drug conjugates wherein both the antibody and drug act on tumors. While the 73JFab was designed to bind to the HER2+ breast cancer cells, the missing Fc region may prevent antibody dependent cell-mediated cytotoxicity (ADCC) [15,50]; however, even a full IgG (73JIgG or the clinically used trastuzumab) would not be efficacious by this mechanism in our immunocompromised mouse model [51].

Achieving more efficacious formulations of docetaxel is critical for clinical use. Here we show that by using a high-load, serum-stable, TBP-modified NP system, we can deliver DTX more effectively and at higher doses compared to a free drug, surfactant based formulation. We expect this strategy of TBP modification to be broadly applicable to other delivery vehicles and not limited to our polymeric nanoparticles. The surfactants used to solubilize these hydrophobic drugs for intravenous formulations are toxic, and associated with a number of adverse reactions in patients. By eliminating the surfactant and using a biocompatible nanoparticle, we are able to increase the dose in NSG mice bearing an orthotopic breast tumor, leading to enhanced survival and reduced tumor burden.

4. Materials & methods

4.1. Free DTX and NP DTX formulations

Free DTX was prepared by dissolving DTX in a mixture of ethanol and polysorbate 80 and then diluting in saline to a final solution of 7.5% polysorbate 80, 10% ethanol, 82.5% saline. The 1.25 mg/mL stock was injected directly or diluted to the desired concentration. P(LA-co-TMCC)-g-PEG-Furan (P_{furan}) and P(LA-co-TMCC)-g-PEG, TBP (P_{TBP}) were synthesized following previously established protocols [21,22]. Briefly, 12000 g/mol backbone is synthesized by a ring opening polymerization of D,L-lactide and 2-methyl-2-carboxy-trimethylene carbonate catalyzed by a thiourea and initiated by a pyrenebutanol. PEG chains are grafted onto the backbone by carbodiimide chemistry, and peptide is conjugated onto backbone using a Michael addition between a thiolated backbone and a maleimide (Mal) modified peptide (Mal-PGFAPLTSRGSQQYAA) [6]. Since both TBP and DTX have limited aqueous solubility, their exact interaction and affinity are difficult to characterize; however, we hypothesize that TBP binds to one DTX and induces drug-drug stacking. The specificity of this interaction was demonstrated with a similarly hydrophobic, scrambled peptide sequence, which had significantly less DTX encapsulated [6]. After purification by dialysis and size exclusion chromatography, polymers were lyophilized and further characterized. Both polymers were characterized by ^{1}H NMR and P_{TBP} was further analyzed by amino acid analysis. For NP DTX formulations, polymer was a mix of 90% P_{TBP} and 10% P_{furan}. NP DTX were formed by co-dissolving polymer (4 mg) and DTX (2.4 mg) in DMF (1 mL) to which 50 μL of borate buffer (pH 9, 500 mM) was added. The solution was left at room temperature for 15 min before 0.5 mL of distilled water was added dropwise. Batches were scaled up to 15 mL of DMF depending on the scale of material needed for individual studies. Scale-up had no impact on drug loading or NP size. Solutions were dialyzed against distilled water for 24 h, changing the water two times (MWCO 2 kg/mol). The solution was centrifuged to remove DTX aggregates prior to use and characterization (5000 rpm, 15 min). Particles were characterized by dynamic light scattering (DLS). DTX concentration was quantified by HPLC-MS/MS using a Waters XTerra C18 column (3.5 μm) on an Agilent 1100 HPLC equipped with an AB

Sciex API 4000 triple quadrupole mass spectrometer with electrospray ionization source detector. Solutions were diluted into 80:20 v/v acetonitrile: water and compared to a DTX standard curve (3.125−200 ng/mL) using paclitaxel as an internal standard (100 ng/mL). NP DTX solutions were lyophilized and stored at −20 °C prior to use. Immediately prior to injection, NP DTX was resuspended in saline to desired concentrations for dosing. Solutions were sonicated in a water bath at 25 °C for 10 min to ensure complete dissolution.

4.2. Cell maintenance and preparation

MDA-MB-231/H2N cells were a generous gift from Dr. Robert Kerbel (Sunnybrook Research Institute, Toronto, ON, Canada). The cells were maintained in house in RPMI 1640 culture medium supplemented with 10% heat-inactivated fetal bovine serum (FBS), 50 units/mL penicillin and 50 μg/mL streptomycin under a humidified 5% CO_2 environment. To prepare cells for injection, cells were rinsed with PBS and detached using trypsin-ethylenediamine tetraacetic acid (trypsin-EDTA). Once suspended, cells were pelleted and washed 3 times in PBS before resuspension at a concentration of 31.25×10^6 cells/mL. Cells were kept on ice prior to injection.

4.3. Orthotopic breast cancer model

The protocols used in these in vivo studies were approved by the University Health Network Animal Care Committee and performed in accordance with current institutional and national regulations. Animals were housed in a 12 h light and 12 h dark cycle with free access to food and water. NOD scid gamma (NSG) mice were bred either in-house (for PK and efficacy study) or purchased from Jackson (for MTD study). 7−9 week old female mice were selected for tumor xeno-transplantation. To form orthotopic mammary fat pad tumors, mice were inoculated with 1.5×10^6 MDA-MB-231-H2N cells suspended in 50 μL of sterile PBS. Prior to surgery, mice were anaesthetized with isoflurane-oxygen. The surgical area was depilated and swabbed with betadine before making an incision in the skin of the lower abdomen to the right of the midline, uncovering the mammary fat pad in the right inguinal region into which the cells were injected. The incision was then sutured closed and lactated Ringer's solution and buprenorphine were given postoperatively for recovery and pain management.

4.4. DTX injections

For all studies, mice were injected through the tail vein with 200 μL of specified formulation using a BD324702 insulin syringe. Syringes were pre-coated with either 0.01% polysorbate 80 in saline (for free DTX formulations) or with 1 mg/mL polymer in saline to prevent drug loss. Syringes were primed to reduce adsorption by drawing and withdrawing solutions 3 times prior to filling with desired formulation.

4.5. Maximum tolerated dose study

Maximum tolerated doses were determined in a dose escalation study between 2 and 10 mg/kg docetaxel. Mice bearing orthotopic MDA-MB-231/H2N tumors (2 weeks post cell impant) were randomized into treatment groups and given three injections at selected doses at days 0, 5 and 8. Mice were monitored daily for weight loss and signs of distress (unresponsive, labored breathing, discharge). At day 15 post-injection, mice were euthanized and organs (tumor, kidney, liver, thigh muscle) were collected for histology (H&E). All sections were examined by a trained pathologist

at the CMDH Pathology Core.

4.6. Pharmacokinetics and biodistribution study

The PK and biodistribution of NP DTX was compared to free DTX at 5 mg/kg in mice 2 weeks post cell implantation (tumors palpable). Groups of 16 mice were randomly assigned to each formulation, with groups being subdivided into three groups of three (terminal end points at 2, 4 and 7 h) and one group of six (terminal end point at 24 h). Mice were placed on a staggered blood sampling schedule (10 min, 30 min, 1, 2, 4, 7 and 24 h) via a femoral blood draw (<30 μL) such that each mouse was sampled for blood no more than three times prior to a terminal cardiac puncture. Blood was collected using EDTA tubes (Sarsdet 16.444.100) and immediately centrifuged to collect the plasma fraction. At terminal time points animals were sacrificed by CO_2 asphyxiation and blood was collected via cardiac puncture. The plasma fraction was immediately isolated by centrifugation. Tissues samples (heart, lung, liver, kidney, spleen, and tumor) were collected by dissection, rinsed in PBS, placed in vials and snap frozen.

4.7. Plasma and tissue preparation

To prepare plasma for quantification by HPLC-MS/MS, samples were thawed and 10 μL was removed and diluted with 10 μL of 1% formic acid in water. To this solution, 10 μL of 100% acetonitrile containing paclitaxel, the internal standard, at 1 μg/mL was added. The sample was vortexed (15 s, 2x) prior to the addition of 70 μL cold acetonitrile. After an additional vortex, samples were centrifuged at 16,000g for 15 min at 4 °C to spin down precipitated protein. Supernatant was removed for quantification by LC-MS/MS as described above.

To prepare the tissues for quantification, samples were thawed, accurately weighed, and 1.0 mm diameter zirconia beads were added to the tubes (~20 beads/tube) to facilitate homogenization. 200 μL of 1% formic acid and 200 μL of acetonitrile containing 500 ng/mL of the internal standard were added. Samples were homogenized for 1 min (2x) using a bead beater, with cooling over ice between homogenization steps. 600 μL of cold acetonitrile was added to the tube, followed by an additional two homogenization steps. Samples were then spun down at 16,000xg for 15 min in the cold room to remove precipitated protein. Supernatant was removed for quantification by LC-MS/MS.

4.8. DTX concentration measurement

Chromatographic separations were carried out using the LC-MS/MS as described in the above section to quantify drug loading. The mobile phase was 0.1% formic acid in water (solvent A) and methanol (solvent B). The column was held for 0.5 min at 50% solvent A, with a drop to 5% over 0.5 min, holding for 0.5 min, and moving back to 50% in 0.1 min, with a final hold for 3.2 min. Docetaxel was quantified by comparing to a docetaxel standard curve (3.125 ng/mL-200 ng/mL), using paclitaxel as an internal standard (100 ng/mL). Docetaxel was monitored at 830.20 and 549.20 m/z; paclitaxel was monitored at 876.20 and 308.10 m/z. When necessary, samples were diluted further to be within the linear standard curve.

4.9. Fab-73J conjugation

Fab-73J was modified with a maleimide (average 1.9 maleimide/Fab quantified using SAMSA fluorescein) using sulfo-SMCC chemistry previously described [15]. Upon resuspension of NP DTX in saline (pH 5.5), 23 μL of a 4.4 μM solution of Fab-73J-maleimide (10

eq to NP) was added to the solution and allowed to react via Diels-Alder (between the Fab-73J-maleimide and PEG-furan) for 4 h prior to injection. We have previously shown using flow cytometry that an average of 10 antibodies/particle results in optimal binding to HER2 over-expressing cells [52]. Previous work has shown the Diels-Alder reaction was confirmed to go to completion at low equivalents using Alexa Fluor-488 labelled Fabs [15], so a purification step (and subsequent loss of drug) can be avoided.

5. Efficacy study

Mice bearing orthotopic MDA-MB-231/H2N tumors were checked biweekly to monitor tumor progression and body weight. When tumors were palpable, mice were randomized into five groups (n = 9) by tumor size and body weight, and treated by intravenous tail vein injection with one of (1) NP Control (6 mg/mL polymer NP in saline) (2) NP DTX (5 mg/kg DTX in the NP, dissolved in saline) (3) Free DTX (5 mg/kg DTX, dissolved in 7.5% polysorbate 80, 10% ethanol in saline) (4) NP DTX (8 mg/kg DTX in the NP, dissolved in saline) (5) Fab-NP DTX (8 mg/kg DTX in the Fab-73J-NP, dissolved in saline) on days 0, 5, and 8. Tumor dimensions and body weight were measured biweekly. The tumor volume was calculated using the formula: $V = (\pi \times (\text{short diameter})^2 \times (\text{long diameter}))/6$. Mice with tumor volumes >1500 mm^3 or weight loss of over 20% were sacrificed.

5.1. PK and statistical analyses

PK parameters were assessed with Phoenix WinNonlin. All statistical analyses were performed using Graph Pad Prism version 5.00 for Macintosh (Graph Pad Software, San Diego, California, www.graphpad.com). Differences among 3 or more groups were assessed by one-way ANOVA with Bonferroni post hoc correction to identify statistical differences among three or more treatments. Analysis of survival curves was done using a Log-rank Mantel-Cox Test. Alpha levels were set at 0.05 and a p value of <0.05 was set as the criteria for statistical significance. Graphs are annotated where p-values are represented as $^*p < 0.05$, $^{**}p < 0.01$, or $^{***}p < 0.001$.

Appendix A. Supplementary data

Supplementary data related to this article can be found at http://dx.doi.org/10.1016/j.biomaterials.2017.01.026.

References

[1] J.E. Cortes, R. Pazdur, Docetaxel, J. Clin. Oncol. 13 (1995) 2643–2655.

[2] A.J. ten Tije, J. Verweij, W.J. Loos, A. Sparreboom, Pharmacological effects of formulation vehicles, Clin. Pharmacokinet. 42 (2003) 665—685, http://dx.doi.org/10.2165/00003088-200342070-00005.

[3] J. Liu, P. Zahedi, F. Zeng, C. Allen, Nano-sized assemblies of a PEG-docetaxel conjugate as a formulation strategy for docetaxel, J. Pharm. Sci-Us 97 (2008) 3274—3290, http://dx.doi.org/10.1002/jps.21245.

[4] F. Alexis, E. Pridgen, L.K. Molnar, O.C. Farokhzad, Factors affecting the clearance and biodistribution of polymeric nanoparticles, Mol. Pharm. 5 (2008) 505—515, http://dx.doi.org/10.1021/mp800051m.

[5] K. Park, Facing the truth about nanotechnology in drug delivery, ACS Nano 7 (2013) 7442—7447, http://dx.doi.org/10.1021/nn404501g.

[6] J. Logie, C.K. McLaughlin, R.Y. Tam, M.S. Shoichet, Innovative use of the taxol binding peptide overcomes key challenges of stable and high drug loading in polymeric nanomicelles, Chem. Commun. 51 (2015) 12000—12003, http://dx.doi.org/10.1039/C5CC04282H.

[7] Y. Shi, M.J. van Steenbergen, E.A. Teunissen, L. Novo, S. Gradmann, M. Baldus, et al., Π—Π stacking increases the stability and loading capacity of thermosensitive polymeric micelles for chemotherapeutic drugs, Biomacromolecules 14 (2013) 1826—1837, http://dx.doi.org/10.1021/bm400234c.

[8] X. Zhao, Z. Poon, A.C. Engler, D.K. Bonner, P.T. Hammond, Enhanced stability of polymeric micelles based on postfunctionalized poly(ethylene glycol)- b-poly(γ-propargyl l-glutamate): the substituent effect, Biomacromolecules 13 (2012) 1315—1322, http://dx.doi.org/10.1021/bm201873u.

[9] C.K. McLaughlin, J. Logie, Core, Corona, Modifications for the design of polymeric micelle drug-delivery systems, Israel J. … 53 (2013) 670—679, http://dx.doi.org/10.1002/ijch.201300085.

[10] Y. Zhao, F. Fay, S. Hak, J. Manuel Perez-Aguilar, B.L. Sanchez-Gaytan, B. Goode, et al., Augmenting drug—carrier compatibility improves tumour nanotherapy efficacy, Nat. Commun. 7 (2016) 11221, http://dx.doi.org/10.1038/ncomms11221.

[11] Y. Shi, R. van der Meel, B. Theek, E. Oude Blenke, E.H.E. Pieters, M.H.A.M. Fens, et al., Complete regression of xenograft tumors upon targeted delivery of paclitaxel viaΠ—Π stacking stabilized polymeric micelles, ACS Nano 9 (2015) 3740—3752, http://dx.doi.org/10.1021/acsnano.5b00929.

[12] J. Lu, S.C. Owen, M.S. Shoichet, Stability of self-assembled polymeric micelles in serum, Macromolecules 44 (2011) 6002—6008, http://dx.doi.org/10.1021/ma200675w.

[13] D.P.Y. Chan, S.C. Owen, M.S. Shoichet, Double click: dual functionalized polymeric micelles with antibodies and peptides, Bioconjugate Chem. 24 (2013) 105—113, http://dx.doi.org/10.1021/bc300511a.

[14] M.X. Sliwkowski, I. Mellman, Antibody therapeutics in cancer, Science 341 (2013) 1192—1198, http://dx.doi.org/10.1126/science.1241145.

[15] S.C. Owen, N. Patel, J. Logie, G. Pan, H. Persson, J. Moffat, et al., Targeting HER2+ breast cancer cells: lysosomal accumulation of anti-HER2 antibodies is influenced by antibody binding site and conjugation to polymeric nanoparticles, J. Control. Release 172 (2013) 395—404, http://dx.doi.org/10.1016/j.jconrel.2013.07.011.

[16] M. Schneider, A. Ny, C.R. de Almodovar, P. Carmeliet, A new mouse model to study acquired lymphedema, PLoS Med. 3 (2006) e264, http://dx.doi.org/10.1371/journal.pmed.0030264.

[17] B.A. Ruggeri, F. Camp, S. Miknyoczki, Animal models of disease: pre-clinical animal models of cancer and their applications and utility in drug discovery, Biochem. Pharmacol. 87 (2014) 150—161, http://dx.doi.org/10.1016/j.bcp.2013.06.020.

[18] M. Das Thakur, N.K. Pryer, M. Singh, Mouse tumour models to guide drug development and identify resistance mechanisms, J. Pathol. 232 (2013) 103—111, http://dx.doi.org/10.1002/path.4285.

[19] M.C. Bibby, Orthotopic models of cancer for preclinical drug evaluation, Eur. J. Cancer 40 (2004) 852—857, http://dx.doi.org/10.1016/j.ejca.2003.11.021.

[20] J.J. Killion, R. Radinsky, I.J. Fidler, Cancer Metastasis Rev. 17 (1998) 279—284, http://dx.doi.org/10.1023/A:1006140513233.

[21] J. Lu, M.S. Shoichet, Self-assembled polymeric nanoparticles of organocatalytic copolymerized d, l-lactide and 2-methyl 2-carboxytrimethylene carbonate, Macromolecules 43 (2010) 4943—4953, http://dx.doi.org/10.1021/ma1004265.

[22] J. Logie, S.C. Owen, C.K. McLaughlin, M.S. Shoichet, PEG-graft density controls polymeric nanoparticle micelle stability, Chem. Mater. 26 (2014) 2847—2855, http://dx.doi.org/10.1021/cm500448x.

[23] M. Shahin, A. Lavasanifar, Novel self-associating poly(ethylene oxide)-b-poly(ε-caprolactone) based drug conjugates and nano-containers for paclitaxel delivery, Int. J. Pharm. 389 (2010) 213—222, http://dx.doi.org/10.1016/j.ijpharm.2010.01.015.

[24] H.-J. Cho, H.Y. Yoon, H. Koo, S.-H. Ko, J.-S. Shim, J.-H. Lee, et al., Self-assembled nanoparticles based on hyaluronic acid-ceramide (HA-CE) and Pluronic® for tumor-targeted delivery of docetaxel, Biomaterials 32 (2011) 7181—7190, http://dx.doi.org/10.1016/j.biomaterials.2011.06.028.

[25] J. Hrkach, D. Von Hoff, M.M. Ali, E. Andrianova, J. Auer, T. Campbell, et al., Preclinical development and clinical translation of a PSMA-targeted docetaxel nanoparticle with a differentiated pharmacological profile, Sci. Transl. Med. 4 (2012), http://dx.doi.org/10.1126/scitranslmed.3003651, 128ra39—128ra39.

[26] K.S. Ho, A.M. Aman, R.S. Al-awar, M.S. Shoichet, Amphiphilic micelles of poly(2-methyl-2-carboxytrimethylene carbonate-co-d,l-lactide)-graft-poly(ethylene glycol) for anti-cancer drug delivery to solid tumours,

Biomaterials 33 (2012) 2223—2229, http://dx.doi.org/10.1016/j.biomaterials.2011.11.072.

[27] M.J. Ernsting, W.-L. Tang, N.W. Maccallum, S.-D. Li, Preclinical pharmacokinetic, biodistribution, and anti-cancer efficacy studies of a docetaxel-carboxymethylcellulose nanoparticle in mouse models, Biomaterials 33 (2012) 1445—1454, http://dx.doi.org/10.1016/j.biomaterials.2011.10.061.

[28] S.C. Kim, D.W. Kim, Y.H. Shim, J.S. Bang, H.S. Oh, S.W. Kim, et al., In vivo evaluation of polymeric micellar paclitaxel formulation: toxicity and efficacy, J. Control. Release 72 (2001) 191—202, http://dx.doi.org/10.1016/S0168-3659(01)00275-9.

[29] S.-W. Lee, M.-H. Yun, S.W. Jeong, C.-H. In, J.Y. Kim, M.H. Seo, et al., Development of docetaxel-loaded intravenous formulation, Nanoxel-PM™ using polymer-based delivery system, J. Control. Release 155 (2011) 262—271, http://dx.doi.org/10.1016/j.jconrel.2011.06.012.

[30] A. Wicki, D. Witzigmann, V. Balasubramanian, J. Huwyler, Nanomedicine in cancer therapy: challenges, opportunities, and clinical applications, J. Control. Release 200 (2015) 138—157, http://dx.doi.org/10.1016/j.jconrel.2014.12.030.

[31] S. Wilhelm, A.J. Tavares, Q. Dai, S. Ohta, J. Audet, H.F. Dvorak, et al., Analysis of nanoparticle delivery to tumours, Nat. Publ. Group 1 (2016) 16014, http://dx.doi.org/10.1038/natrevmats.2016.14.

[32] C.M. Dawidczyk, C. Kim, J.H. Park, L.M. Russell, K.H. Lee, M.G. Pomper, et al., State-of-the-art in design rules for drug delivery platforms: lessons learned from FDA-approved nanomedicines, J. Control. Release 187 (2014) 133—144, http://dx.doi.org/10.1016/j.jconrel.2014.05.036.

[33] W.J. Gradishar, Phase III trial of nanoparticle albumin-bound paclitaxel compared with polyethylated Castor oil-based paclitaxel in women with breast cancer, J. Clin. Oncol. 23 (2005) 7794—7803, http://dx.doi.org/10.1200/JCO.2005.04.937.

[34] H. Maeda, L.W. Seymour, Y. Miyamoto, Conjugates of anticancer agents and polymers: advantages of macromolecular therapeutics in vivo, Bioconjugate Chem. 3 (1992) 351—362, http://dx.doi.org/10.1021/bc00017a001.

[35] U. Prabhakar, H. Maeda, R.K. Jain, E.M. Sevick-Muraca, W. Zamboni, O.C. Farokhzad, et al., Challenges and key considerations of the enhanced permeability and retention effect for nanomedicine drug delivery in oncology, Cancer Res. 73 (2013) 2412—2417, http://dx.doi.org/10.1158/0008-5472.CAN-12-4561.

[36] J.W. Nichols, Y.H. Bae, EPR: evidence and fallacy, J. Control. Release 190 (2014) 451—464, http://dx.doi.org/10.1016/j.jconrel.2014.03.057.

[37] T. Lammers, L.Y. Rizzo, G. Storm, F. Kiessling, Personalized nanomedicine, Clin. Cancer Res. 18 (2012) 4889—4894, http://dx.doi.org/10.1158/1078-0432.CCR-12-1414.

[38] T. Miller, S. Breyer, G. van Colen, W. Mier, U. Haberkorn, S. Geissler, et al., Premature drug release of polymeric micelles and its effects on tumor targeting, Int. J. Pharm. 445 (2013) 117—124, http://dx.doi.org/10.1016/j.ijpharm.2013.01.059.

[39] M.N. Khalid, P. Simard, D. Hoarau, A. Dragomir, J.-C. Leroux, Long circulating poly(ethylene glycol)-decorated lipid nanocapsules deliver docetaxel to solid tumors, Pharm. Res. 23 (2006) 752—758, http://dx.doi.org/10.1007/s11095-006-9662-5.

[40] C.C. Milsom, C.R. Lee, C. Hackl, S. Man, R.S. Kerbel, Differential post-surgical metastasis and survival in SCID, NOD-SCID and NOD-SCID-IL-2Rγnull mice with parental and subline variants of human breast cancer: implications for host defense mechanisms regulating metastasis, PLoS One 8 (2013), http://dx.doi.org/10.1371/journal.pone.0071270 e71270.

[41] G. Shen, R. Xing, N. Zhang, C. Chen, G. Ma, X. Yan, Interfacial cohesion and assembly of bioadhesive molecules for design of long-term stable hydrophobic nanodrugs toward effective anticancer therapy, ACS Nano 10 (2016) 5720—5729, http://dx.doi.org/10.1021/acsnano.5b07276.

[42] H. Lee, H. Fonge, B. Hoang, R.M. Reilly, C. Allen, The effects of particle size and molecular targeting on the intratumoral and subcellular distribution of polymeric nanoparticles, Mol. Pharm. 7 (2010) 1195—1208, http://dx.doi.org/10.1021/mp100038h.

[43] K.F. Pirollo, E.H. Chang, Does a targeting ligand influence nanoparticle tumor localization or uptake? Trends Biotechnol. 26 (2008) 552—558, http://dx.doi.org/10.1016/j.tibtech.2008.06.007.

[44] A.T. Florence, "Targeting" nanoparticles: the constraints of physical laws and physical barriers, J. Control. Release 164 (2012) 115—124, http://dx.doi.org/10.1016/j.jconrel.2012.03.022.

[45] M. Ahmed, D.W. Pan, M.E. Davis, Lack of in vivo antibody dependent cellular cytotoxicity with antibody containing gold nanoparticles, Bioconjugate Chem. 26 (2015) 812—816, http://dx.doi.org/10.1021/acs.bioconjchem.5b00139.

[46] D.B. Kirpotin, Antibody targeting of long-circulating lipidic nanoparticles does not increase tumor localization but does increase internalization in animal models, Cancer Res. 66 (2006) 6732—6740, http://dx.doi.org/10.1158/0008-5472.CAN-05-4199.

[47] N. Kamaly, Z. Xiao, P.M. Valencia, A.F. Radovic-Moreno, O.C. Farokhzad, Targeted polymeric therapeutic nanoparticles: design, development and clinical translation, Chem. Soc. Rev. 41 (2012) 2971, http://dx.doi.org/10.1039/c2cs15344k.

[48] J.D. Heidel, M.E. Davis, Clinical developments in nanotechnology for cancer therapy, Pharm. Res. 28 (2010) 187—199, http://dx.doi.org/10.1007/s11095-010-0178-7.

[49] Y. Chen, X. Zhu, X. Zhang, B. Liu, L. Huang, Nanoparticles modified with tumor-

targeting scFv deliver siRNA and miRNA for cancer therapy, Mol. Ther. 18 (2010) 1650–1656, http://dx.doi.org/10.1038/mt.2010.136.

[50] R. Nahta, F.J. Esteva, Herceptin: mechanisms of action and resistance, Cancer Lett. 232 (2006) 123–138, http://dx.doi.org/10.1016/j.canlet.2005.01.041.

[51] C.A. Hudis, Trastuzumab — mechanism of action and use in clinical practice, N. Engl. J. Med. 357 (2007) 39–51, http://dx.doi.org/10.1056/NEJMra043186.

[52] K. Ho, Y. Lapitsky, M. Shi, M.S. Shoichet, Tunable immunonanoparticle binding to cancer cells: thermodynamic analysis of targeted drug delivery vehicles, Soft Matter 5 (2009) 1074, http://dx.doi.org/10.1039/b814204a.